Colloids and Surfaces B: Biointerfaces 143 (2016) 243–251

Contents lists available at ScienceDirect

Colloids and Surfaces B: Biointerfaces

journal homepage: www.elsevier.com/locate/colsurfb

Peptide-incorporated 3D porous alginate scaffolds with enhanced osteogenesis for bone tissue engineering

Zuyuan Luo[a,b], Yue Yang[c], Yi Deng[b], Yuhua Sun[a], Hongtao Yang[d], Shicheng Wei[a,b,*]

[a] Second Dental Center, Central Laboratory, School and Hospital of Stomatology, Peking University, Beijing 100081, China
[b] Center for Biomedical Materials and Tissue Engineering, Academy for Advanced Interdisciplinary Studies, Peking University, Beijing 100871, China
[c] Department of Stomatology, Xuanwu Hospital, Capital Medical University, Beijing 00053, China
[d] Department of Materials Science and Engineering, College of Engineering, Peking University, Beijing 100871, China

ARTICLE INFO

Article history:
Received 1 December 2015
Received in revised form 1 March 2016
Accepted 16 March 2016
Available online 17 March 2016

Keywords:
3D porous scaffolds
Alginate
Bioactivity
Peptide
Bone tissue engineering

ABSTRACT

Good bioactivity and osteogenesis of three-dimensional porous alginate scaffolds (PAS) are critical for bone tissue engineering. In this work, alginate and bone-forming peptide-1 (BFP-1), derived from bone morphogenetic protein-7 (BMP-7), have been combined together (without carbodiimide chemistry treatment) to develop peptide-incorporated PAS (p-PAS) for promoting bone repairing ability. The mechanical properties and SEM images show no difference between pure PAS and p-PAS. The release kinetics of the labeled peptide with 6-carboxy tetramethyl rhodamine from the PAS matrix suggests that the peptide is released in a relatively sustained manner. In the cell experiment, p-PAS show higher cell adhesion, spreading, proliferation and alkaline phosphatase (ALP) activity than the pristine PAS group, indicating that the BFP-1 released from p-PAS could significantly promote the aggregation and differentiation of osteoblasts, especially at 10 μg/mL of trapped peptide concentration (p-PAS-10). Furthermore, p-PAS-10 was implanted into Beagle calvarial defects and bone regeneration was analyzed after 4 weeks. New bone formation was assessed by calcein and Masson's trichrome staining. The data reveal that p-PAS group exhibits significantly enhanced oseto-regenerative capability *in vivo*. The peptide-modified PAS with promoted bioactivity and osteogenic differentiation *in vitro* as well as bone formation ability *in vivo* could be promising tissue engineering materials for repairing and regeneration of bone defects.

1. Introduction

For repairing bone defects and regenerating bone function, autologous and allogenic bone are still being considered as "gold standard" in clinic [1–3]. However, the drawbacks of this methodology, including donor site morbidity, hematomas, inflammation and second surgical sites with associated morbidity, as well as the high cost of bone-harvesting procedures, have already compelled researchers to seek for alternatives *via* tissue engineering [4,5]. Tissue engineering to address limitations in tissue grafting is becoming more and more important for a wide variety of orthopedic diseases. The concept of tissue engineering is to transplant a bio-factor (cells, genes and/or proteins) within a porous degradable material known as a scaffold [6]. Far from being a passive component, scaffold material and three-dimensional (3D) porous architecture design (here architecture refers to features 10–1000 μm in size) play a significant role in tissue regeneration by preserving tissue volume, providing temporary mechanical function, and delivering bio-factors [6–8].

Materials used for preparing scaffolds for bone tissue engineering should meet requirements such as biocompatibility and osteoconductive [9–12]. Alginate is one of the best-known biocompatible and biodegradable nature polymers, composing of guluronic acid and mannuronic acid. It is widely used for growth factor delivery, cell encapsulation and as the porous scaffolds in bone loss or failure treatment [13–18]. Alginate forms stable hydrogels in the presence of certain di- or trivalent cations (e.g., Ca^{2+} and Ba^{2+}) at low concentrations through the ionic interaction between the cations and the carboxyl functional group of guluronic acid units located on the polymer chain [19,20]. The porous alginate scaffolds (PAS) could be prepared facilely by freeze-drying method [21–23]. The confined osteogenesis ability of bare PAS has hampered their direct usage in bone regenerative medicine. However, they still hold the potential for being used in bone tissue engineering for excellent biocompatibility and the capability of delivery a bio-factor. A

* Corresponding author at: Second Dental Center, Central Laboratory, School and Hospital of Stomatology, Peking University, Beijing 100081, China.
E-mail addresses: sc-wei@pku.edu.cn, weishicheng99@163.com (S. Wei).

http://dx.doi.org/10.1016/j.colsurfb.2016.03.047
0927-7765/

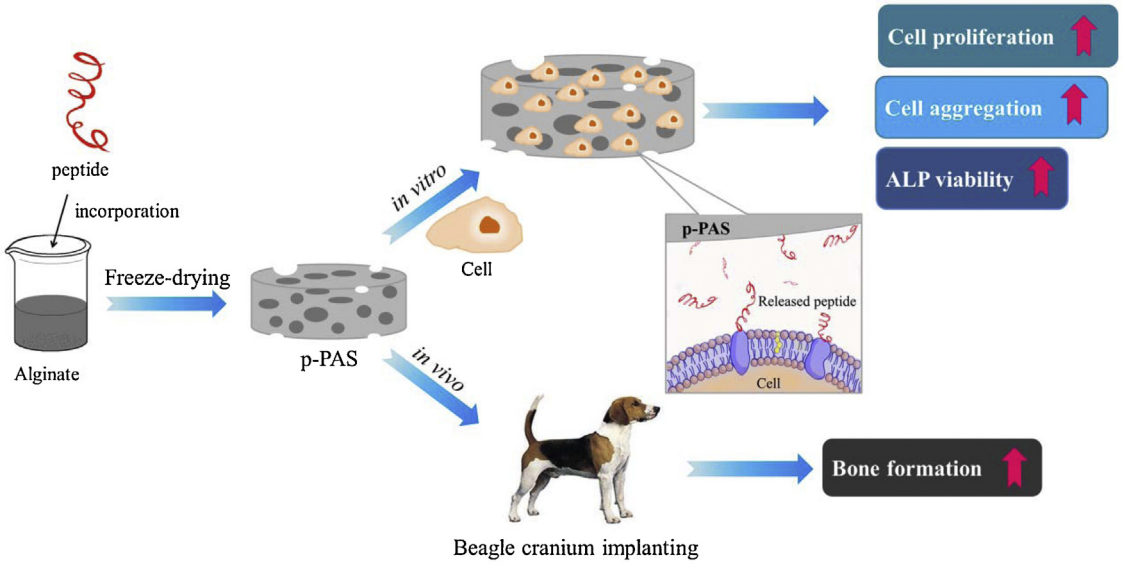

Scheme 1. Schematic illustration of preparation of the peptide-incorporated PAS and effect of the modified p-PAS on cells *in vitro* and on Beagle calvarial defects *in vivo*.

great deal of effort has been devoted to enhance the bioactivity of PAS. For instance, introducing the hydroxyapatite (HA) powders into PAS was reported to mimic the native extracellular matrix of bone [10,24–27]. Direct mixing, however, is usually lack of control and results in inhomogeneity of particle distribution in the alginate matrix with limited bioactivity. Incorporating chitosan into PAS to form chitosan-alginate porous scaffolds seemly had achieved better distribution [12,28]. Nevertheless, these studies had not imitated the *in vivo* natural osteogenesis microenvironment including bone growth factors which is very effective in repairing bone defects [12]. Another approach is to incorporate the osteogenic proteins, such as bone morphogenetic proteins (BMPs) family, into the PAS to facilitate the bone formation in a controlled and sustained way [6,29,30]. Although the growth factor released from BMPs/PAS could mimic the osteo-microenvironment and promote the new bone formation, the complex multilevel structure of BMPs renders it prone to degradation, and tends to lose their bioactivity quickly in physiological conditions [31]. Therefore, peptides from the BMPs have currently attracted an extensive attention due to their small structure, minimal or no side-effect, as well as no immunogenicity compared to larger proteins [32]. Recently, Kim demonstrated that a new peptide sequence (GQGFSYPYKAVFSTQ) from the immature region of the BMP-7, named bone-forming peptide-1 (BFP-1), could induce osteo-differentiation and proliferation with higher osteogenic activity than BMP-7 [33,34]. Our previous study also confirmed that the BFP-1 delivered by mesoporous silica nanoparticles (MSNs) could enhance the proliferation, spreading and alkaline phosphatase (ALP) activity of MG-63 cells [35]. Simultaneously, the osteogenesis-related proteins expression and calcium mineral deposition disclose stimulated osteo-differentiation of human mesenchymal stem cells (hMSCs) [35].

The beneficial effect of the bone-forming peptide mentioned above has motivated us to incorporate the growth factor into PAS to promote the bone forming ability of the scaffolds. To the best of our knowledge, there are no reports on investigating the impregnation of osteogenic peptide into 3D porous scaffolds *in vitro*, as well as on facilitating the regenerative repair of defects *in vivo*. As shown in Scheme 1, we have fabricated facile 3D peptide-incorporated porous alginate scaffolds (p-PAS) without using carbodiimide chemistry treatment, and characterized the structure as well as the release kinetics of peptide. Moreover, the cell proliferation and osteogenic differentiation activity *in vitro* as well as bone formation ability *in vivo* for pure PAS and p-PAS with different peptide-incorporated concentrations were also compared and investigated.

2. Materials and methods

2.1. Materials

Sodium alginate (SA) with high molecular weight ($M_w \approx 100{,}000$) and high mannuronic acid content ($G/M \approx 0.64$) was purchased from Sigma-Aldrich (A2033, St. Louis, USA). The bone forming peptide-1 (BFP-1, GQGFSYPYKAVFSTQ sequence) and the 6-carboxy tetramethyl rhodamine-labeled (TAMRA-labeled) BFP-1 provided by China Peptides Co., Ltd. (Shanghai, China), both were synthesized by a batch-wise fmoc-poly-amide method to more than 98% purity. All other chemicals were of analytical reagent grades and were used as received unless noted. All aqueous solutions were prepared with de-ionized water (D.I. water).

2.2. Fabrication of pure and peptide-incorporated porous alginate scaffolds (p-PAS)

3.0 g of alginate powder was dissolved and thoroughly mixed in 100 mL of D.I. water. The alginate solution was adjusted to pH 7.4 by adding acetic acid drop-wise. Peptide was then loaded into the alginate solutions and agitated for 1 h at 4 °C to obtain the peptide-alginate solutions with the final concentrations of 1, 10, and 100 μg/mL respectively. These solutions were then introduced into 24-well cell culture plates (1 mL per well) and maintained in a freezer at −20 °C for 24 h. The samples were then lyophilized in a freeze dryer (VDF-2000A, Boyikang, China) at 0.1 Torr (shelf temperature −20 °C) for another 24 h. The dried porous scaffolds were cross-linked with 1% (w/v) $CaCl_2$ (Sigma-Aldrich, USA) solution for 10–15 min, washed twice, and immersed in D.I. water overnight to remove unbound $CaCl_2$. Later, the specimens were freeze-dried for 24 h again to obtain the peptide-incorporated porous alginate scaffolds. All the samples were kept dry in a freezer at −20 °C until sterilization. Based on different concentrations of peptide in alginate solutions (1, 10 and 100 μg/mL), the prepared peptide-incorporated porous alginate scaffolds were denoted as p-PAS-1, p-PAS-10 and p-PAS-100 respectively.

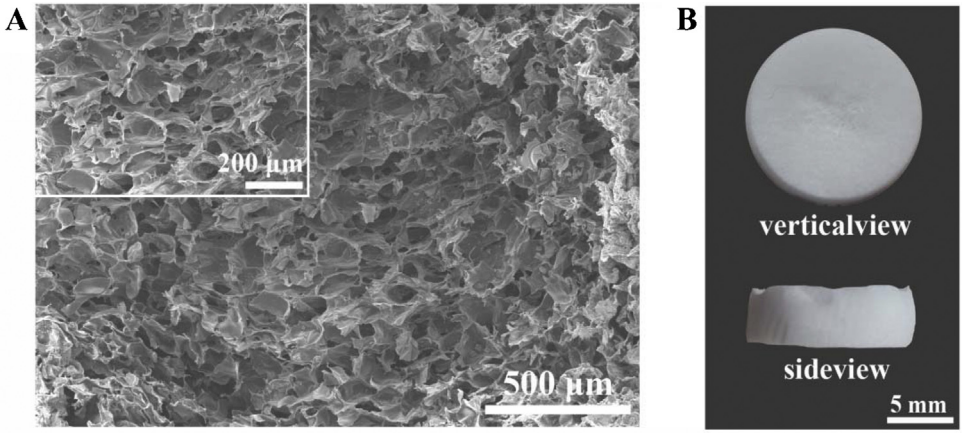

Fig. 1. The SEM image (A), and photograph (B) of p-PAS.

2.3. Characterization

The interconnected porous structures of scaffolds were observed using a field emission scanning electron microscope (S-4800, Hitachi, Japan). Measurements were performed in triplicate. The compressive mechanical strength and modulus of scaffolds were tested using a mechanical tester (5969, Instron, USA) with 50 kN load cells following the guidelines in ASTM D5024-95a [36]. The crosshead speed of the tester was set at 0.4 mm/min until the samples were compressed to about 30% of their initial thickness [12].

2.4. Peptide release from porous scaffold

The release profiles of peptide from p-PAS were assessed using a fluorescence spectrophotometer (Enspire 2300-100L, PerkinElmer, USA). The 6-carboxy tetramethyl rhodamine (TAMRA) labeled BFP-1 incorporated PAS (TB-PAS) were first prepared. Briefly, TAMRA-labeled BFP-1 was added into the alginate solutions and agitated at 4 °C with the final concentrations of the labeled peptide at 10 and 100 μg/mL. The method used to synthesize TB-PAS is consistent with that presented in "2.2. Fabrication of pure and peptide-incorporated porous alginate scaffolds (p-PAS)". However, the TB-PAS should be kept in a dark container at −20 °C. Subsequently, each sample was immersed in 10 mL of PBS (pH 7.4, 37 °C) for up to 21 days, respectively. At the pre-determined time points (1, 3, 5, 7 and 24 h, and 2–11, 14, 16, 18–21 days), 100 μL of supernatant was collected for calculation of the peptide released in solution using the fluorescence spectrophotometer. The concentration of peptide was calculated by comparison with the established standard curve obtained from the unlabeled peptide.

2.5. Cell culture

Human osteoblast-like MG-63 cells (American Type Culture Collection, VA, USA) were cultured in Dulbecco's modified Eagle medium (DMEM) (Invitrogen Life Technologies, Carlsbad, USA) containing 10% fetal bovine serum (Gibco, Carlsbad, USA), 1% (v/v) streptomycin (Amresco, Cleveland, USA), and 1% (v/v) penicillin (Amresco) at 37 °C in a humidified atmosphere of 5% CO_2. The cell medium was changed every 2–3 days.

2.6. Cell viability

All the scaffolds were sterilized by immersing in a 75% alcohol solution for 30 min and then air-dried overnight. Before cell seeding, the samples were washed with PBS thrice and immersed in 24-well plates (Costar, USA) with DMEM containing 10% fetal bovine serum (FBS) for 48 h. Then, 5×10^4 MG-63 cells in 1 mL DMEM were seeded on PAS, p-PAS-1, p-PAS-10 and p-PAS-100, respectively. In addition, 5×10^4 MG-63 cells in 1 mL 10% (v/v) DMSO DMEM medium was added into empty wells as positive control. The cell counting kit-8 assay (CCK-8, Dojindo, Japan) was used to evaluate the viability of cells. Briefly, after 1, 3, 7 and 14 days incubation, 100 μL of CCK-8 was added into each well for 3 h incubation, and the absorbance value of supernatant optical density (OD value) was measured with a microplate reader (Model 680, Bio-Rad, CA) at a 450 nm wavelength.

2.7. Morphology and cytoskeletal observation

The morphology and cytoskeletal of cells cultured on scaffolds were examined by a field emission scanning electron microscope (S-4800, Hitachi, Japan) and confocal laser scanning microscopy (A1R-si, Nikon, Japan) after 7 days, respectively. For SEM observation, scaffolds were fixed in 2.5% glutaraldehyde solution for 1 h and then dehydrated in ascending concentrations of ethanol for 30 min each. Dehydrated samples were dried by a vacuum dryer, and examined under SEM. For confocal laser scanning microscopy (CLSM) observation, cells were washed with PBS and fixed with 4% (w/v) paraformaldehyde for 30 min. The samples were then permeabilized with 0.5% (v/v) Triton X-100 (Sigma) for 5 min, and stained with 5 μg/mL FITC-phalloidin solution (Sigma-Aldrich) for 30 min. After washed with PBS, samples were incubated for 10 min at room temperature with 10 μg/mL DAPI solution (Sigma-Aldrich).

2.8. Alkaline phosphatase (ALP) activity assay

MG-63 cells were cultured on PAS and p-PAS with different incorporated peptide concentrations under the same conditions described above. After culture for 7 and 14 days the medium was removed and 1 mL of 0.1% TritonX-100 (v/v) was added into each well and incubated for 1 h. Then the cell-lysis solution was collected and centrifuged (12000 rpm, 4 °C) for 30 min to remove all cell debris. Afterwards, 30 μL of supernatant was transferred to a new 96-well plate for ALP determination according to the manufacturer's instructions (Nanjing Jiancheng Biotechnology, China). For normalization, the total protein concentration was measured by a Bicinchoninic Acid (BCA) protein assay kit (Pierce 23227, Thermo, USA).

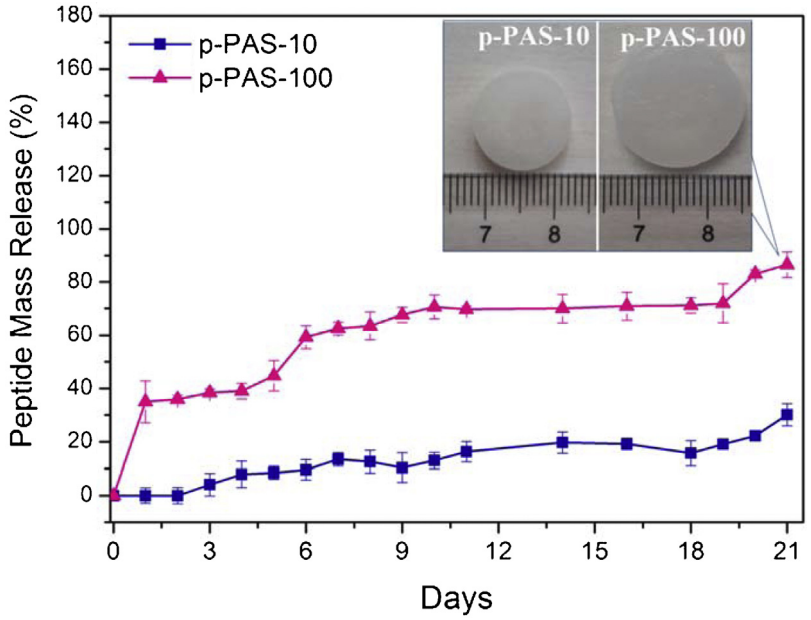

Fig. 2. BFP-1 peptide release behavior from p-PAS; and the photographs of p-PAS after releasing 21 days. Data are reported as the mean ± SD of triplicate experiments.

2.9. In vivo *study*

To probe the *in vivo* bone formation of p-PAS-10, male Beagle dogs aged 1.5 years and weighing 12.8 ± 1.3 kg were chosen to create bone defect model. The animals were divided into 3 groups: blank control (defected-only), PAS and p-PAS-10. Briefly, PAS and p-PAS-10 debris were transplanted into a 1.2 cm diameter non-critical-size defect in cranium. After surgery, a fluorochrome (Sigma-Aldrich), calcein (50 mg/kg) was administered to assess the osteogenic activity of the scaffolds at 4 weeks. These Beagles were sacrificed after implantation for 4 weeks with intravenous injection of 10% kalium chloratum (0.5 mL/kg), respectively.

2.10. Histological analysis

At 4 weeks post-implantation, calvarias were harvested intact, and fixed in 4% paraformaldehyde for 24 h at 4 °C, and then ultrathin sections were obtained for histologic detection. Briefly, tissue samples were fixed in 10% neutral buffered formalin for 7 days, and the bones were embedded in methyl methacrylate resin and sectioned with a microtome (SP1600, Leica, Germany). The tissue sections were ground to a thickness of 30 μm and the fluorochrome new bone marker label was detected using CLSM. Subsequently, longitudinal sections were prepared and treated with Masson's trichrome to examine the new bone formation.

2.11. Statistical analysis

All data were expressed as mean ± standard deviations of a representative six experiments. Statistical analysis was performed by one-way analysis of variance (ANOVA) followed by Tukey's post hoc tests using SPSS 19.0 and *p*-values less than 0.05 were considered statistically significant.

3. Results and discussion

3.1. Material characterization

Fig. 1A shows SEM images of the cross sections of the peptide-incorporated p-PAS-10. These scaffolds are highly porous with a pore size around 100–300 μm, which is favorable for cell attachment and new bone tissue ingrowth [37–39]. No visible difference was detected between the morphologies for pure PAS and p-PAS with different incorporated peptide concentrations (data not shown), which indicates that the peptide interfusion has no influence on pore size of the scaffolds. Higher magnification image exhibits porous structures and reveals the porous interconnectivity of PAS. As shown in Fig. 1B, the diameter and thickness of peptide-incorporated porous alginate scaffolds are about 12 ± 0.12 mm and 3 ± 0.06 mm respectively.

Porous scaffolds for bone repairing must have appropriate mechanical strength to sustain bone regeneration at the site of implantation and maintain sufficient integrity during both *in vivo* and *in vitro* cell growth [40–42]. To further determine the impact to PAS after the incorporation of peptide, the mechanical property of p-PAS has been tested. Curves in Fig. S1A, show compression tests results of PAS and p-PAS with different incorporated peptide concentrations (1, 10 and 100 μg/mL). Young's modulus calculated from the curves of PAS, p-PAS-1 and p-PAS-10 are 3.80 ± 0.59 MPa, 3.43 ± 0.60 MPa, and 2.92 ± 0.19 MPa (Fig. S1B) respectively. However, the Young's modulus of p-PAS-100 is 1.50 ± 0.23 MPa and is lower than other groups. The reason could be attributed to that in the high concentration of peptide incorporated p-PAS system there are larger amounts of carboxylate groups (COO^-) from peptide that could capture the Ca^{2+} [43–45], resulting fewer cross-linking density in p-PAS-100.

3.2. The release behavior of p-PAS

Delivery of a growth factor, like bone-forming peptide, alone to a defect will not function well due to its rapid clearance [46]. However, incorporating the BFP-1 into PAS have made it possible to retain the growth factor at the defect site and mimic its temporal profile during bone regeneration *in vivo* through controlled and sustained delivery of growth factor. The cumulative release profiles versus time for p-PAS (Fig. 2) exhibit a long-term continuous-release of incorporated peptide, suggesting sustained peptide delivery behavior of the p-PAS. However, the difference in the velocity of peptide release is observed from the curves of p-PAS-10 and p-PAS-100, which indicates that the release capacity

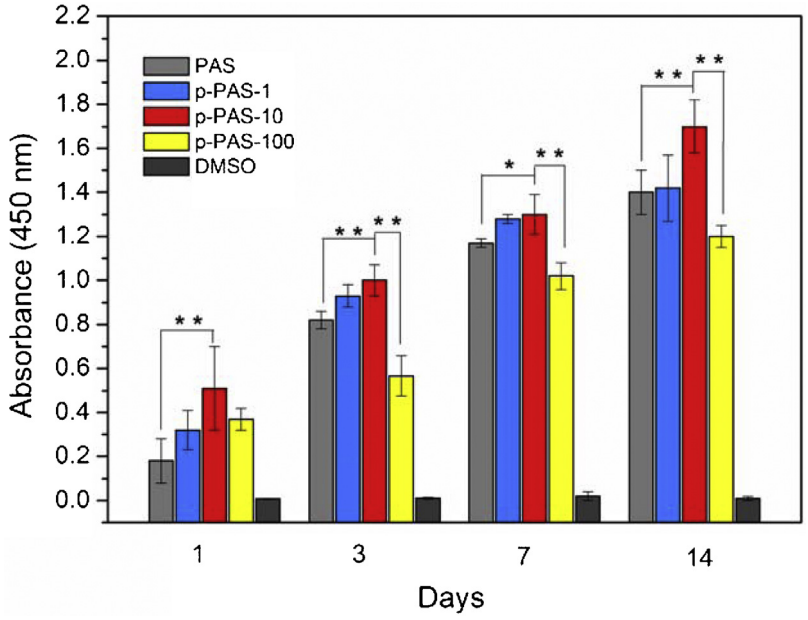

Fig. 3. The cell proliferation rates of MG-63 cells cultured for 1, 3, 7 and 14 days, with the pristine PAS and p-PAS with different incorporated peptide concentrations. * represents $p < 0.05$, ** represents $p < 0.01$.

could be dependent on the concentration of peptide-trapped. Furthermore, peptide molecules are almost completely released (70%) from the p-PAS-100 in the first 9 days. Nevertheless, the p-PAS-10 presents slower drug release patterns, and approximately 30% dose of peptide is released in a relatively sustained rate and lasted for more than 21 days. The reason for the difference between the two samples could be attributed to that there might be a larger amount of peptide molecules on the surface of p-PAS with high encapsulated peptide concentration, causing in the burst release of peptide in p-PAS-100 system. In addition, less cross-linking in p-PAS-100 could lead to an increase in the degradation rate of the scaffolds based on the results in Fig. S1. As shown in the photographs (Fig. 2), the size of p-PAS-100 is much larger than that of p-PAS-10 after 21 days' immersion due to the faster degradation rate of p-PAS-100. The peptide molecules will be released with the degradation of scaffolds, which could also give rise to the quick-release of BFP-1 in p-PAS-100 system.

3.3. In vitro *cytotoxicity evaluation*

Potential cytotoxicity of the as-prepared samples to human osteoblasts is a critical factor for the novel peptide encapsulated porous alginate scaffolds to be used in biomedical applications. Fig. 3 shows cell proliferation rates of the MG-63 cells co-cultured with pristine PAS, p-PAS-1, p-PAS-10 and p-PAS-100 in DMEM for 1, 3, 7 and 14 days, respectively. It suggests that the bare PAS and all p-PAS show no toxicity and all are biocompatible for use as potential bone regenerative repairing materials. However, the cells cultured on p-PAS-10 show outstanding cell viability than all other groups at each time point, indicating that the p-PAS with 10 μg/mL of incorporated peptide could facilitate the proliferation of MG-63 cells remarkably. Nevertheless, p-PAS-100 inhibits the viability of cells, especially after 3, 7 and 14 days' co-culture. These cell viability results could be attributed to the different peptide amount delivered from the p-PAS. The amount of BFP-1 released from p-PAS was calculated based on the release curves in Fig. 2 and the results were shown in Fig. S2. About 0.5 μg/mL and 40 μg/mL peptide in 24-well plates are delivered from p-PAS-10 and p-PAS-100 at the 3rd day, respectively. Previous reports suggested that the concentration of BFP-1 at 1–3 μg/mL could enhance the proliferation of osteoblasts significantly, and high BFP-1 concentration could inhibit the proliferation of cells [33,35]. Hence due to the high concentration of the released peptide, the viability of cells cultured on p-PAS-100 is restrained. On the other hand, only about 3 μg/mL peptides are released from p-PAS-10 at the 21st day, which leads to better cell viability by forming a sustained favorable culture environment.

3.4. *Cellular morphology and cytoskeletal observation*

In order to further confirm the biocompability of p-PAS, the adherent morphologies of osteoblasts were examined. Fig. 4A shows the morphologies of MG-63 cells on the PAS, p-PAS-1, p-PAS-10 and p-PAS-100 observed by SEM at different magnifications after cultured for 7 days. Compared with that of pristine PAS counterpart, cells on peptide-incorporated p-PAS show an elongated morphology with good adherence and spreading. Additionally, from the enlarged images, it can be seen that the MG-63 cells on p-PAS-10 gather together and form cell clusters while the others randomly attach on the surface. Moreover, the fluorescence images from Fig. 4B reveal that numerous cell clusters on p-PAS (especially p-PAS-10) exhibiting actin fibers, suggesting that the released peptide from p-PAS could obviously induce the formation of multicellular aggregation. Furthermore, with enhanced cell adhesion, cells cultured with p-PAS-10 group extend more adhered filopodia and spread more with visible presentation of more mature F-actin intracellular stress fibers. However, the behavior of cells (spreading, adhesion and aggregation) on p-PAS-100 is poorly developed with thin morphology and small quantity (Fig. 4A and B). These results could be attributed to the different peptide content delivered from the p-PAS, consistent with the CCK-8 assay result in Fig. 3. The released peptide from p-PAS-10 have promoted the cell adhesion and proliferation, and the 3D porous structure has provided available space for cells to aggregate [6]. However, according to the result in Fig. 2, within 7 days' co-culture p-PAS-100 might start to degrade, which is adverse to the adhesion of cells. The multicellular aggregation *in vitro* could resemble the bone tissue *in vivo*, which reminders that p-PAS-10 may facilitate the formation of the new bone in defects.

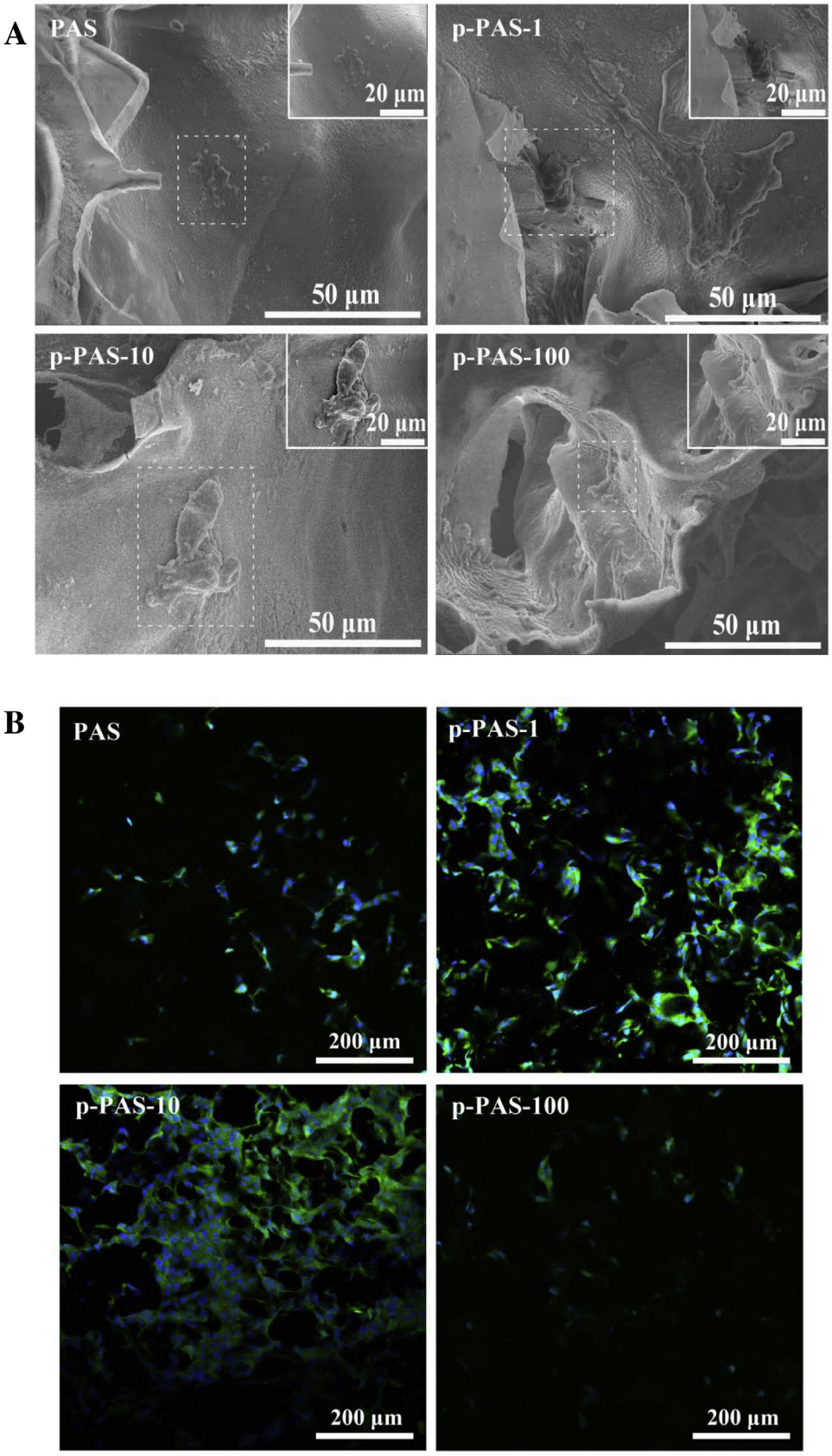

Fig. 4. SEM images (A) and CLSM images of morphology and actin cytoskeletal organization (B) (green, labeled with FITC-phalloidin, counter-stained with DAPI for nuclei in blue) of MG-63 cells after 7 day incubation on pristine PAS and p-PAS. (For interpretation of the references to colour in this figure legend, the reader is referred to the web version of this article.)

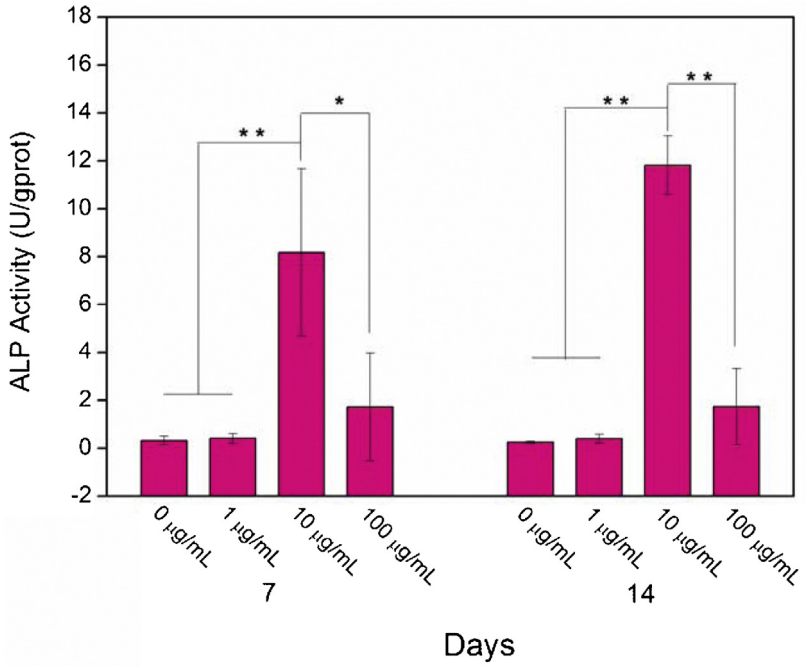

Fig. 5. ALP activity of MG-63 cells on pure PAS and p-PAS with different incorporated peptide concentrations after cultivating for 7 and 14 days, respectively* represents $p < 0.05$ and ** represents $p < 0.01$.

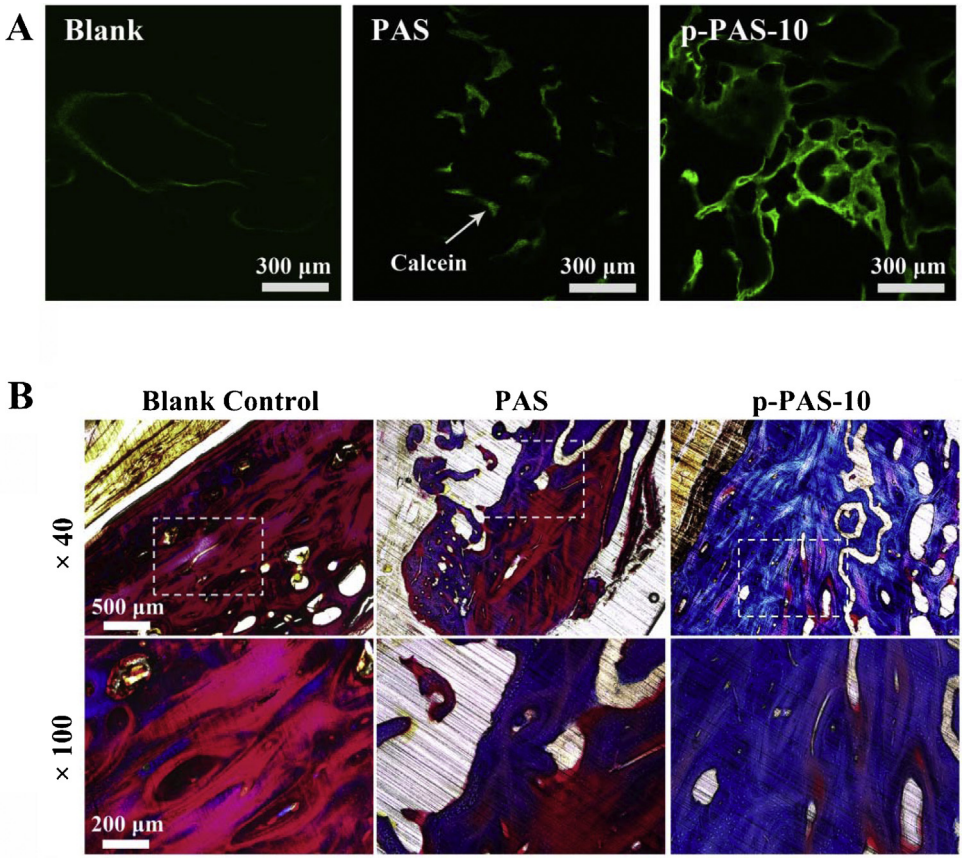

Fig. 6. Histological analysis of regenerated bones in calvarial defects with the immunohistochemical staining of newly-formed bone by calcein (A) and Masson's trichrome staining (B) 4 weeks after surgery.

3.5. Alkaline phosphatase (ALP) activity

Besides cell proliferation and morphology, high osteogenic differentiation activity of bone cells is momentous to p-PAS. Therefore, the osteoblastic phenotypic expression of the peptide-incorporated p-PAS should be examined. The ALP activity, as a significant quantitative marker of bone formation and a considerable indication of osteoblasts expressed in their differentiation phase at 7–14 days [47,48], was tested with MG-63 cells at 7 and 14 days. As shown in Fig. 5, remarkable difference is not found for the ALP production in bare PAS, p-PAS-1 and p-PAS-100 at 7 and 14 days. Nevertheless, ALP activity is significantly increased in cells cultured on p-PAS-10 compared with that of the other groups. These suggest that when the concentration of encapsulated BFP-1 is 10 μg/mL, the amount of the released peptide molecules is optimal to trigger the osteogenic pathway of osteoblasts. As mentioned above, BFP-1 peptide derived from the immature region of BMP-7 protein holds the similar osteogenic induction property, and may bind to the same functional sites (BMP receptors) and induce the up-regulation of target bone-related genes through Smads or mitogen-activated protein kinase (MAPK) [49], therefore facilitating bone formation. Additionally, the high ALP activity of osteoblasts cultured on p-PAS-10 could be attributed to the BFP-1 being delivered in a relatively sustained rate. These results suggest p-PAS-10 hold outstanding bioactivities in cell proliferation, adhesion, aggregation and osteogenesis *in vitro* and it is trustworthy to further study its bone regenerative repairing ability *in vivo*.

3.6. In vivo *bone formation on p-PAS*

To preferably apply p-PAS as an ideal bone repairing material, high bone regeneration ability *in vivo* is desired. Hence, p-PAS specimens were implanted into the cranial bone defects of Beagle dogs (Fig. S2) and the new bone formation and development were evaluated at 4 weeks after surgery. As shown in Fig. 6A, the fluorochrome new bone marker label (calcein) is clearly observed in the regions of defects and plentiful bone deposition and remodeling are found on PAS and p-PAS-10 specimens, suggesting that the 3D porous architecture could increase new bone formation. However, more calcein labeling (green) observed in defects filled with p-PAS-10 indicates that the encapsulated peptide has obviously enhanced bone regeneration ability of 3D porous alginate scaffolds. Based on *in vitro* CLSM results in Fig. 4B, p-PAS-10 has induced the aggregation of osteoblasts, which might promote the growth of new bony tissue. Additionally, remarkable bone regeneration by the p-PAS-10 is also demonstrated by means of Masson's trichrome staining. Fig. 6B shows a significant difference in the extent of blue blocks in p-PAS-10 group and the other two groups. In Masson's trichrome staining, blue staining is indicative of collagen, which is seen in both fibrous connective tissue and osteoid [28]. Osteoid is the organic portion of the bone matrix that forms before the maturation of bone tissue, and is composed of type 1 collagen and chondroitin sulfate as well as osteocalcin [50]. Notably, peptide-incorporated p-PAS-10 greatly facilitates osteoid deposition, which could benefit from the bone formation activity of BFP-1 released from the scaffold. Our peptide-incorporated porous alginate scaffolds (p-PAS-10) have shown high biocompatibility and osteogenesis and have remarkably enhanced bone regeneration *in vivo*. It could have great potential for various bone repairing and tissue engineering applications.

4. Conclusion

Three-dimensional (3D) porous alginate scaffolds are promising materials for bone tissue engineering due to its biocompatibility and degradable properties, as well as the controllable porosity. However, the poor cell adhesion and low osteogenesis ability have limited their capability for bone regeneration *in vivo*. To overcome these deficiencies, we have successfully developed bone forming peptide-incorporated 3D porous alginate scaffolds (p-PAS) incorporated with bone-forming peptide-1 to promote bone-repairing ability. SEM images show a 3D interconnecting porous structure of p-PAS (pore size 100–300 μm), which is beneficial for growing new bone tissue. The release profiles suggest that p-PAS have excellent sustained-release performance. p-PAS-10, in particular, provided sufficient peptide concentrations over 21 days *in vitro* with very continuous and steady release rate. The peptide-trapped PAS positively affected cell adhesion, proliferation and aggregation towards MG-63 cells *in vitro*. At the encapsulated BFP-1 concentration of 10 μg/mL, p-PAS-10 exhibited outstanding bioactivities. Additionally, p-PAS has further elevated the ALP expression of MG-63, which proved that the biological activity of the peptide released from p-PAS could be maintained and BFP-1 could substantially enhance the osteogenic differentiation of osteoblasts. Moreover, after implanting scaffolds into the Beagle calvarial defects for 4 weeks, fluorochrome new bone marker label and Masson's trichrome staining revealed active bone regeneration for p-PAS-10 group. The BFP-1 released from the scaffold had enhanced bone regeneration. Therefore, the peptide-incorporated PAS possess great potential as bioactive composite and drug-delivery vehicle in bone repairing and tissue engineering.

Acknowledgments

This work was supported by Beijing Natural Science Foundation (No. 7132124) and Peking University's 985 Grant.

Appendix A. Supplementary data

Supplementary data associated with this article can be found, in the online version, at http://dx.doi.org/10.1016/j.colsurfb.2016.03.047.

References

[1] E. Sachlos, J. Czernuszka, Eur. Cells Mater. 5 (2003) 29.
[2] E. Monaco, M. Bionaz, S. Hollister, et al., Theriogenology 75 (2011) 1381.
[3] V.M. Betz, O.B. Betz, M.B. Harris, et al., Front. Biosci. 13 (2008) 833.
[4] E.D. Arrington, W.J. Smith, H.G. Chambers, et al., Clin. Orthop. Relat. Res. 329 (1996) 300.
[5] J.D. Kretlow, S. Young, L. Klouda, et al., Adv. Mater. 21 (2009) 3368.
[6] S.J. Hollister, Nat. Mater. 4 (2005) 518.
[7] H. Yoshimoto, Y. Shin, H. Terai, et al., Biomaterials 24 (2003) 2077.
[8] D.W. Hutmacher, Biomaterials 21 (2000) 2529.
[9] T. Coviello, P. Matricardi, C. Marianecci, et al., J. Control. Release 119 (2007) 5.
[10] H.R. Lin, Y.J. Yeh, J. Biomed. Mater. Res. B: Appl. Biomater. 71 (2004) 52.
[11] X. He, Y. Liu, X. Yuan, et al., PLoS One 9 (2014) e104061.
[12] Z. Li, H.R. Ramay, K.D. Hauch, et al., Biomaterials 26 (2005) 3919.
[13] C. Du, J. Zhao, J. Fei, et al., Chem. Asian J. 8 (2013) 736.
[14] W. Cui, Y. Cui, J. Zhao, et al., J. Mater. Chem. B 1 (2013) 1326.
[15] H.H. Tønnesen, J. Karlsen, Drug Dev. Ind. Pharm. 28 (2002) 621.
[16] M. George, T.E. Abraham, J. Control. Release 114 (2006) 1.
[17] I. Freeman, S. Cohen, Biomaterials 30 (2009) 2122.
[18] K.Y. Lee, D.J. Mooney, Prog. Polym. Sci. 37 (2012) 106.
[19] H. Zheng, Carbohydr. Res. 302 (1997) 97.
[20] G.T. Grant, E.R. Morris, D.A. Rees, et al., FEBS Lett. 32 (1973) 195.
[21] S. Zhang, F. Cui, S. Liao, et al., J. Mater. Sci. Mater. Med 14 (2003) 641.
[22] M.H. Ho, P.Y. Kuo, H.J. Hsieh, et al., Biomaterials 25 (2004) 129.
[23] F.J. O'Brien, B.A. Harley, I.V. Yannas, et al., Biomaterials 25 (2004) 1077.
[24] G. Turco, E. Marsich, F. Bellomo, et al., Biomacromolecules 10 (2009) 1575.
[25] M. Petrovic, B. Colovic, V. Jokanovic, et al., J. Ceram. Process. Res. 13 (2012) 398.
[26] R. Dittrich, G. Tomandl, F. Despang, et al., J. Am. Ceram. Soc. 90 (2007) 1703.
[27] J. Venkatesan, I. Bhatnagar, P. Manivasagan, et al., Int. J. Biol. Macromol. 72 (2015) 269.
[28] S.J. Florczyk, M. Leung, Z. Li, et al., J. Biomed. Mater. Res. A 101 (2013) 2974.
[29] M. Weber, A. Steinert, A. Jork, et al., Biomaterials 23 (2002) 2003.
[30] P. Yilgor, K. Tuzlakoglu, R.L. Reis, et al., Biomaterials 30 (2009) 3551.

[31] J. Lock, H. Liu, Int. J. Nanomed. 6 (2011) 2769.
[32] L. Mendes, S. Saska, M. Martines, et al., Mater. Sci. Eng. C: Mater. Biol. Appl. 33 (2013) 4427.
[33] H.K. Kim, J.H. Kim, D.S. Park, et al., Biomaterials 33 (2012) 7057.
[34] Y.J. Lee, J.H. Lee, H.J. Cho, et al., Biomaterials 34 (2013) 5059.
[35] Z. Luo, Y. Deng, R. Zhang, et al., Colloids Surf. B: Biointerfaces 131 (2015) 73.
[36] Y. Zhang, M. Zhang, J. Biomed. Mater. Res. 55 (2001) 304.
[37] K. Whang, K. Healy, D. Elenz, et al., Tissue Eng. 5 (1999) 35.
[38] S. Yang, K.F. Leong, Z. Du, et al., Tissue Eng. 7 (2001) 679.
[39] M.C. Wake, C. Patrick Jr., A. Mikos, Cell Transplant. 3 (1993) 339.
[40] B. Porter, J. oldham, S.L. He, et al., J. Biomech. Eng. 122 (2000) 286.
[41] R.C. Thomson, M.J. Yaszemski, J.M. Powers, et al., J. Biomater. Sci. Polym. Ed. 7 (1996) 23.
[42] T.M.G. Chu, D.G. Orton, S.J. Hollister, et al., Biomaterials 23 (2002) 1283.
[43] M. Nara, H. Torii, M. Tasumi, J. Phys. Chem. 100 (1996) 19812.
[44] N. Huebsch, P.R. Arany, A.S. Mao, et al., Nat. Mater. 9 (2010) 518.
[45] O. Chaudhuri, S.T. Koshy, C.B. da Cunha, et al., Nat. Mater. 13 (2014) 970.
[46] L.C. Gerstenfeld, D.M. Cullinane, G.L. Barnes, et al., J. Cell. Biochem. 88 (2003) 873.
[47] S. Hattar, A. Berdal, A. Asselin, et al., Eur. Cell Mater. 4 (2002) 61.
[48] Q. Li, M. Li, P. Zhu, et al., J. Mater. Chem. 22 (2012) 20257.
[49] H. Senta, H. Park, E. Bergeron, et al., Cytokine Growth Factor Rev. 20 (2009) 213.
[50] D.W. Lee, K.T. Koo, Y.J. Seol, et al., J. Periodontal Implant Sci. 40 (2010) 132.